

SINGLE PULSE IMAGING

S.D. Blunt*, A.K. Shackelford[†], K. Gerlach[†]

*Dept. of Electrical Engineering & Computer Science, University of Kansas, Lawrence, KS

[†]Radar Division, U.S. Naval Research Laboratory, Washington, DC

Keywords: radar imaging, adaptive pulse compression, Doppler processing

Abstract

A novel radar receiver processing technique is presented which utilizes the Doppler phase shift resulting from high-speed targets to produce a range/Doppler image from the return signal of a single radar pulse. Denoted as Single Pulse Imaging (SPI), this technique utilizes the general framework of the Multistatic Adaptive Pulse Compression (MAPC) algorithm and applies it to monostatic radar in which Doppler-shifted realizations of the transmitted waveform are treated as different waveforms that have illuminated different range profiles thereby resulting in the superposition of different signals at the receiver. The joint separation and pulse compression of the set of received signals produces a range/Doppler image whereby, given sufficient disparity in radial velocity (and thus sufficient Doppler phase-shift diversity), individual scatterers within the same range cell can be discerned.

1 Introduction

Radar imaging techniques, such as inverse synthetic aperture radar (ISAR), rely on the Doppler phase shifts induced by relative motion between a target and the radar to generate a range/Doppler image of the target. High range resolution is achieved using pulse compression techniques, whereas high Doppler resolution relies on the accurate measurement of the Doppler shifts induced by uniform rotational motion of the target. In traditional ISAR processing, multiple pulses over a period of time are typically processed using a Fourier transform to measure the various Doppler shifts induced by the motion of the target. If target scatterers move out of their range cells during the imaging time (range walking) or if the rotational motion is not uniform, the image will be smeared. Therefore, motion compensation algorithms must be used to produce a focused ISAR image. Much research has been conducted on the development of robust motion compensation techniques (for example [4]-[6]).

Recently, an adaptive approach based on Reiterative Minimum Mean-Square Error (RMMSE) estimation known as Adaptive Pulse Compression (APC) was developed [7]-[9] and evaluated via simulation. For the monostatic radar case APC is capable of almost completely mitigating range sidelobes thereby enabling estimation of the range profile illuminated by a radar to within the accuracy of the noise, thus facilitating the detection of very small power targets when in the presence of nearby large targets. The elimination of range sidelobes is accomplished by adaptively estimating the appropriate receiver pulse compression filter to use for each individual range cell. The filters place nulls in the location of large scatterers, suppressing the sidelobes they would otherwise generate. The adaptive filters are obtained via a bootstrapping operation, where matched filter range cell estimates are utilized as an initial estimate of the range profile. Furthermore, APC has been shown to be superior to mismatched filtering based upon Least Squares estimation. The APC approach has been generalized to perform shared-spectrum multistatic radar reception in a manner analogous to spread-spectrum communications systems. This algorithm, denoted as Multistatic Adaptive Pulse Compression (MAPC) [1]-[3], adaptively estimates a unique pulse compression filter for each individual range cell of each illuminated range profile for which a reflected signal is received.

Here, we present a technique for measuring the Doppler frequency shift of fast moving/maneuvering targets from a single transmitted pulse using a Doppler-sensitive variation of the MAPC algorithm. In the next section the received signal model is presented, followed by a description of the new adaptive processing technique, and finally simulation results are shown.

2 Received Signal Model

We begin the derivation of the SPI algorithm by first considering a simplistic scenario where all of the scatterers are moving at the same velocity, r , relative to the radar platform. The motion relative to the radar platform induces a Doppler phase shift, θ , in the received signal for each scatterer. The length- N vector \mathbf{s} denotes the discrete-time version of the transmitted waveform. The length- N vector

$\mathbf{x}(l, \theta) = [x(l, \theta) \ x(l-1, \theta) \ \dots \ x(l-N+1, \theta)]$ represents a set of N contiguous samples of the range profile impulse response with which the transmitted waveform convolves. Note that the range profile is a function of θ , highlighting the fact that all of the scatterers in the range profile are moving at the same relative velocity and therefore induce the same Doppler phase shift θ in the radar return signal. The l^{th} sample of the received radar return is defined as

$$y(l, \theta) = (\mathbf{x}(l, \theta) \circ \mathbf{p}(\theta))^T \mathbf{s} + v(l), \quad (1)$$

for, $l = 0, \dots, L+N-2$, where \circ indicates element by element multiplication (also known as the Hadamard product). The N -length vector $\mathbf{p}(\theta) = [1 \ e^{j\theta} \ e^{j2\theta} \ \dots \ e^{j(N-1)\theta}]^T$ contains the relative phase shifts of the N contiguous samples of $\mathbf{x}(l, \theta)$ where θ here is defined as the Doppler phase shift between successive received samples.

Although the received signal model of (1) is for scatterers moving at the same relative velocity, the model can easily be generalized to include scatterers moving at many velocities by integrating (1) over all possible Doppler phase shifts. The l^{th} sample of the total received signal is then

$$y(l) = \int_{-\pi}^{\pi} (\mathbf{x}(l, \theta) \circ \mathbf{p}(\theta))^T \mathbf{s} \, d\theta + v(l). \quad (2)$$

Although (2) is continuous in θ , it can be approximated to within a scale factor by

$$y(l) = \sum_{k=1}^K (\mathbf{x}(l, \theta_k) \circ \mathbf{p}(\theta_k))^T \mathbf{s} + v(l), \quad (3)$$

where

$$\theta_k = -\pi + \frac{2\pi}{K-1}(k-1), \quad k = 1, \dots, K, \quad (4)$$

and K is arbitrarily large, such that (3) is a good approximation of (2). For notational simplicity, we denote $\mathbf{x}(l, \theta_k) \triangleq \mathbf{x}_k(l)$. By rearranging terms, (3) can be expressed as

$$y(l) = \sum_{k=1}^K \mathbf{x}_k^T(l) \tilde{\mathbf{s}}_k + v(l), \quad (5)$$

where

$$\tilde{\mathbf{s}}_k = \mathbf{s} \circ \mathbf{p}(\theta_k) \quad (6)$$

is a Doppler phase-shifted version of the transmitted waveform. The collection of N samples of the received

return signal $\mathbf{y}(l) = [y(l) \ y(l+1) \ \dots \ y(l+N-1)]^T$ can therefore be expressed as

$$\mathbf{y}(l) = \sum_{k=1}^K \mathbf{X}_k^T(l) \tilde{\mathbf{s}}_k + \mathbf{v}(l), \quad (7)$$

where

$$\mathbf{X}_k(l) = [\mathbf{x}_k(l) \ \mathbf{x}_k(l+1) \ \dots \ \mathbf{x}_k(l+N-1)] \\ = \begin{bmatrix} x_k(l) & x_k(l+1) & \dots & x_k(l+N-1) \\ x_k(l-1) & x_k(l) & & x_k(l+N-2) \\ \vdots & \vdots & \ddots & \vdots \\ x_k(l-N+1) & x_k(l-N+2) & \dots & x_k(l) \end{bmatrix}. \quad (8)$$

As shown by (7), a radar return from multiple targets with varying velocities can be approximately expressed as a summation of the returns from K distinct stationary range profiles, each illuminated by a unique waveform $\tilde{\mathbf{s}}_k$. By moving the Doppler phase shift $\mathbf{p}(\theta_k)$ from the return signal to the waveform, the signal model has been transformed from being monostatic with a composite range profile to being multistatic in which the distinct range profiles may be separable. The signal model given by (7) is mathematically identical to that used for derivation of the MACP algorithm given co-aligned angles of arrival for the K received signals [1]–[3]. Hence, using the MAPC formulation and solution, the SPI algorithm is able to accurately estimate each “range profile”, thereby producing an estimate of the two-dimensional range-Doppler profile. By measuring both range and Doppler information of multiple targets using a single pulse, it is possible to produce focused radar images without the use of complicated motion compensation techniques. Note, however, that the Doppler resolution is limited by the length of the pulse and therefore SPI maybe appropriate only for high-speed maneuvering targets.

Because the target Doppler shifts are not known *a priori*, a bank of filters consisting of phase shifted versions of the transmitted waveform is utilized in the receiver to accommodate all of the possible Doppler shifts. These phase shifted versions of the transmitted waveform partition the Doppler space such that regardless of the Doppler shift induced by target motion, the radar return will match closely to at least one of the waveforms in the receiver. In order to facilitate the greatest Doppler resolution, a waveform with a thumbtack type ambiguity function should be utilized for transmission. Because the ambiguity peak is narrow in both range and Doppler, the range/Doppler “location” of a given target can be more accurately measured than would be possible for a Doppler-tolerant waveform, such as a linear FM waveform. Ideally, by using phase-shifted versions of a

thumbtack waveform, the return from a non-stationary target will only closely match to a single waveform in the receiver.

3 Single Pulse Imaging

Were one to use a bank of standard matched filters, the range profile for the k^{th} Doppler shift could be estimated as

$$\hat{x}_{MF,k}(l) = \tilde{\mathbf{s}}_k^H \mathbf{y}(l). \quad (9)$$

However, due to high range sidelobes and the inherent correlation between nearby Doppler phase-shift vectors, the bank of matched filters would be unable to accurately distinguish between targets based on their Doppler shifts, as will be demonstrated in the next section. To overcome the issues of range sidelobes and Doppler correlation, the bank of matched filters $\tilde{\mathbf{s}}_k$ in (9) is replaced by a bank of range adaptive RMMSE-based filters. To produce an estimate of the received range profile associated with a particular Doppler, an MMSE cost function [10] is minimized for each range cell of each ‘‘range profile’’ as

$$J_k(l) = E \left[\left| x_k(l) - \mathbf{w}_k^H(l) \mathbf{y}(l) \right|^2 \right], \quad (10)$$

where $\mathbf{w}_k(l)$ is the APC weight vector for the l^{th} range cell in the k^{th} range profile which is associated with Doppler phase shift θ_k . The solution to (10) takes the form [1]-[3]

$$\mathbf{w}_k(l) = \hat{\rho}_k(l) \left(\sum_{i=1}^K \mathbf{C}_i(l) + \mathbf{R} \right)^{-1} \tilde{\mathbf{s}}_k, \quad (11)$$

where $\hat{\rho}_k(l) = |\hat{x}_k(l)|^2$ is the estimated power of $x_k(l)$, $\mathbf{R} = E[\mathbf{v}(l) \mathbf{v}(l)^H]$ is the noise covariance matrix, and the i^{th} signal correlation matrix is given by

$$\mathbf{C}_i(l) = \sum_{n=-N+1}^{N-1} \hat{\rho}_k(l+n) \tilde{\mathbf{s}}_{i,n} \tilde{\mathbf{s}}_{i,n}^H, \quad (12)$$

where $\tilde{\mathbf{s}}_{i,n}$ contains the elements of the Doppler phase-shifted waveform $\tilde{\mathbf{s}}_i$ shifted by n samples and zero-filled in the remaining n samples, e.g.

$$\tilde{\mathbf{s}}_{i,2} = \left[0 \ 0 \ \tilde{s}_i(0) \ \cdots \ \tilde{s}_i(N-3) \right]^T \quad \text{and}$$

$$\tilde{\mathbf{s}}_{i,-2} = \left[\tilde{s}_i(2) \ \cdots \ \tilde{s}_i(N-1) \ 0 \ 0 \right]^T.$$

Estimates of the K range profiles, as well as knowledge of the noise covariance matrix \mathbf{R} are required to form the weight vectors \mathbf{w}_k . The range profiles are estimated in bootstrapping fashion through reiterative application of the

SPI filter bank. Assuming the noise covariance is white Gaussian, \mathbf{R} simplifies to $\sigma_v^2 \mathbf{I}_N$, where σ_v^2 is the noise power, and \mathbf{I}_N is the $N \times N$ identity matrix. Initial estimates of the range profiles can be obtained simply by applying the bank of matched filters as in (9). These estimates can be employed in (11) to estimate the adaptive filters which may then be used to update the range profile estimates. This reiterative procedure is applied for a predetermined number of stages, with each stage improving the accuracy of the estimates. It has been found via simulation that 4-6 stages of reiteration are needed to achieve good suppression of the range/Doppler sidelobes. The structure of the SPI filter bank enables fast implementation via the matrix inversion lemma through a straightforward extension of the approach utilized in [9].

The Doppler resolution obtained when using SPI is approximately $\frac{\pi}{N}$, therefore finer Doppler resolution can be achieved by increasing the length of the transmitted waveform. Although the observed Doppler resolution implies that the adaptive filter bank should include approximately $K = 2N$ phase shifted waveforms (one filter for each Doppler cell over 2π), it has been found through simulation that at least $K = 10N$ phase shifted waveforms are required for good sidelobe suppression performance. The large number of required filters is a result of using a thumbtack waveform. Due to the narrowness of the waveform’s ambiguity peak, thumbtack waveforms are rather intolerant to Doppler shifts; a small Doppler phase shift results in a mismatch thus limiting the range/Doppler sidelobe suppression capability. Therefore, the Doppler space must be partitioned very finely in order to minimize this mismatch.

4 Simulation Results

The performance of the SPI algorithm is assessed by comparing the output of SPI to that of a bank of matched filters for two simulated target scenarios. For both test cases, the transmit waveform \mathbf{s} is an $N = 30$ random polyphase waveform.

The first example is a simulated target scenario consisting of a large stationary target surrounded by four smaller targets in noise. Two of the smaller targets are stationary, located 7 range cells before and after the large target. The other two small targets are in the same range cell as the large target, but are non-stationary with Doppler phase shifts of ± 0.3 radians per received sample (analogous to Mach 2 targets illuminated by a $3.5\text{-}\mu\text{s}$ pulse at W-band). The signal-to-noise ratio (SNR) of the large target is 30 dB, and the small targets are 15 dB lower than the large target. The image produced from a bank of matched filters is shown in Fig. 1, and the SPI image is shown in Fig. 2. The only identifiable

target when the bank of matched filters is utilized is the large stationary target with all other targets masked by its range and Doppler sidelobes. However, all five targets are easily identifiable in the SPI image.

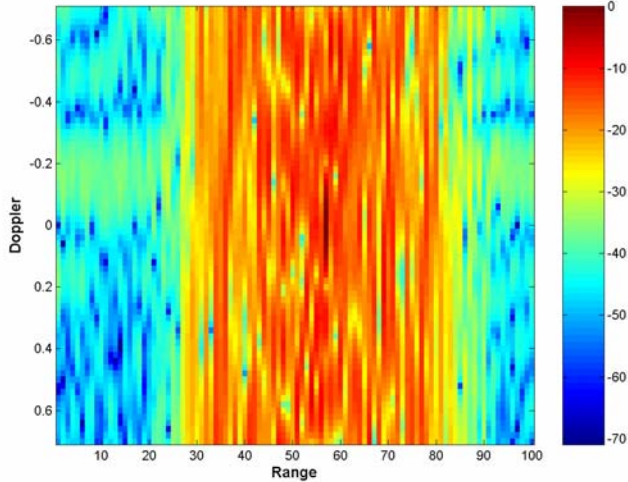


Fig. 1. Range-Doppler image for matched filter bank

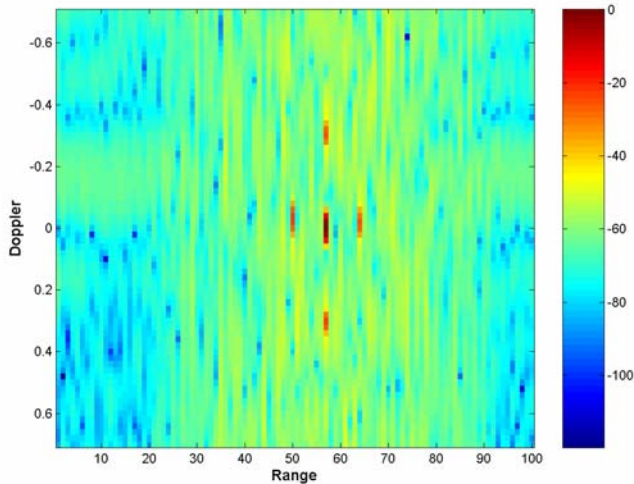


Fig. 2. Range-Doppler image for SPI

The second test case consists of two equal strength targets at the same range cell but with differing Doppler shifts. The SNR of the targets is 40 dB. One of the targets is stationary and the other target has a Doppler shift of 0.1 radians per received signal sample. For a length $N = 30$ transmitted waveform, the two targets are separated by approximately $\frac{\pi}{N}$ radians, the expected Doppler resolution of the SPI algorithm. The outputs of the matched filter bank and SPI are both illustrated in Fig. 3, where a cross section across Doppler is shown for the range cell containing the two

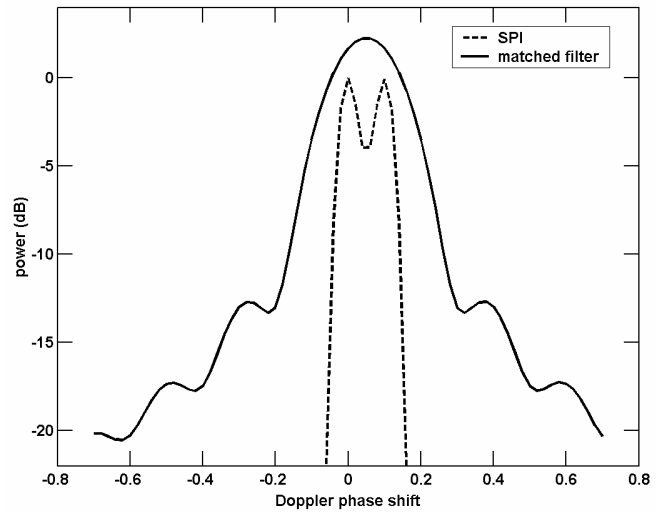


Fig. 3. Doppler profile of SPI and matched filter bank for two scatterers at the same range cell with differing Dopplers

targets. While the two targets appear as a single target in the output of the matched filter bank, they are clearly distinguishable using the SPI algorithm.

5 Conclusions

In the formulation for the SPI algorithm, Doppler phase shifts induced by high speed targets are modeled as having been produced by a set of Doppler-shifted versions of the transmitted waveform each reflected by its own individual range profile. As such, the Doppler-shifted returns from high-speed targets can be represented as a multistatic scenario in which the set of range profiles can be combined to produce a range/Doppler image not unlike a bank of matched filters. However, because the matched filters are known to be susceptible to high range and Doppler sidelobes, the SPI algorithm utilizes a technique inspired by the MAPC algorithm such that the sidelobes can be adaptively suppressed. Simulation results indicate that, to within the limits of range/Doppler resolution, it is possible to provide accurate estimates of small targets that would otherwise be masked by the sidelobes of nearby larger targets.

6 Acknowledgement

This work was supported by the United States Office of Naval Research (ONR 31).

7 References

- [1] S. D. Blunt, and K. Gerlach, "Joint adaptive pulse compression to enable multistatic radar," *IEE*

Waveform Diversity and Design Conf., Edinburgh, Scotland, (2004).

- [2] S. D. Blunt, and K. Gerlach, "Aspects of multistatic adaptive pulse compression," *IEEE Intl. Conf. on Radar*, Arlington, Virginia, pp. 104-108, (May 2005).
- [3] S. D. Blunt, and K. Gerlach, "Multistatic adaptive pulse compression," *IEEE Trans. on Aerospace and Electronic Systems*, vol. 42, no. 1, (Jan. 2006).
- [4] J. S. Son, G. Thomas, and B. C. Flores, *Range-Doppler Radar Imaging and Motion Compensation*, Artech House, pp. 9-19, (2001).
- [5] V. C. Chen, and S. Qian, "Joint time-frequency transform for radar range-Doppler imaging," *IEEE Trans. on Aerospace and Electronic Systems*, Vol. 34, No. 2, pp. 486-499, (April 1998).
- [6] F. Berizzi, E. Dalle Mese, M. Diani, and M. Martorella, "High-resolution ISAR imaging of Maneuvering targets by means of the range instantaneous Doppler technique: modelling and performance analysis," *IEEE Trans. Image Processing*, Vol. 10, No. 12, pp. 1880-1890, Dec. 2001.
- [7] S. D. Blunt, and K. Gerlach, "A novel pulse compression scheme based on minimum mean-square error reiteration," *IEEE Intl. Conf. on Radar*, Adelaide, Australia, pp. 349-353, (Sept. 2003).
- [8] S. D. Blunt, and K. Gerlach, "Adaptive pulse compression," *IEEE National Radar Conf.*, Philadelphia, Pennsylvania, pp. 271-276, (April 2004).
- [9] S. D. Blunt, and K. Gerlach, "Adaptive pulse compression via MMSE estimation," *IEEE Trans. on Aerospace and Electronic Systems*, in press.
- [10] S.M. Kay, *Fundamentals of Statistical Signal Processing: Estimation Theory*, Upper Saddle River, NJ: Prentice-Hall, pp. 219-286 & pp. 344-350, (1993).